

MUC-NOTE-COOL_THEORY-233

Muon Tech. Note MU-046

Revision 1

The Effects of Different Cooling Materials and Windows

R. B. Palmer, R. Fernow, J. Gallardo

Brookhaven National Laboratory

Upton, New York, 11973

March 5, 2002

Abstract

The equilibrium emittances and rates of cooling are calculated for different materials, windows and foils. A comparison with ICOOL[5] shows that these calculations give good estimates of simulated cooling in a given lattice. Assuming that the use of hydrogen will require a second safety window twice as thick as the containment window, then it is shown that the performance of hydrogen is almost the same as helium with no such safety window, and very little better than that with lithium hydride and no containment.

ICOOL simulations are shown for the full Study 2[1] cooling channel. The addition of the safety window reduces the $\frac{\mu}{p}$ ratio by 9%. The use of helium (without safety window), or LiH (with no window), both give about 5% less cooling than that for hydrogen with a safety window.

It is also shown that grids of tubes (80% coverage) with 25 μm (1 mil) aluminum walls would give the same scattering as the Study 2 beryllium windows.

1 Introduction

To meet safety requirements, one, or even two, stronger safety windows may be required between the hydrogen (H) absorbers and the rf. This note explores the consequences of adding such material and looks at alternatives of helium (He) and lithium hydride (LiH). Note that the density of *LiH* in ICOOL is $\rho_{LiH} = 0.82 \frac{\text{g}}{\text{cm}^3}$; a search of the literature has shown that a better value is $0.78 \frac{\text{g}}{\text{cm}^3}$ [2].

2 Calculation

Using the energy loss dE/dz (absolute value), radiation length L_R , the beta-tron function β_{\perp} , and thicknesses of materials in a cooling channel, we can calculate the expected equilibrium emittances. If only one material is present then the equilibrium emittance is [3]:

$$\epsilon_{\text{equilib}} = \beta_{\perp} F(E) Q(\text{mat}) \quad (1)$$

where

$$F(E) = \left(\frac{1}{\beta_v \frac{(dE/dz)}{(dE/dz)_{\min}}} \right), \quad Q(\text{mat}) = \left(\frac{E_s^2}{2 m_{\mu} c^2 L_R (dE/dz)_{\min}} \right), \quad (2)$$

and $E_s \approx 14.1$ MeV, $m_{\mu} c^2 = 105.6$ MeV, and all other units are mks.

$F(E)$ for our cases is close to unity. Values of $Q(\text{mat})$, and other constants, are given in Tb. 1.

For a channel containing several different materials with different lengths and local $\beta_{\perp i}$'s, one can define an effective $Q'(\text{mat})$ as a function of the individual lengths, $\beta_{\perp i}$'s, L_{Ri} 's and $(dE/dz)_i$'s:

$$Q'(\text{mat}) = \left(\frac{E_s^2}{2 m_{\mu} c^2} \right) \left(\frac{\sum_i^n \left(\frac{\beta_{\perp i}}{\beta_{\perp}} \right) \frac{1}{L_{Ri}} \Delta \ell_i}{\sum_i^n \left(\frac{dE}{dz} \right)_i \Delta \ell_i} \right). \quad (3)$$

For the primary absorber and its windows we assume that the local $\beta_{\perp i}$ varies with distance ℓ from the absorber center as (β_o is the local beta at the center of the absorber)

$$\beta_{\perp i} \approx \beta_o + \frac{\ell^2}{\beta_o} \quad (4)$$

Table 1: Energy loss, radiation length, Q values and other parameters for the absorber materials and windows considered in this paper. [4]

Material	K_{cond} (J/s m K)	T_{melt} (C)	$(dE/dz)_{\text{min}}$ (MeV/cm)	L_R (cm)	$Q(\text{mat})$ (mm mrad/cm)
Liq. H ₂	0.10		0.286	865	38
Liq. He	0.02		0.242	755	52
LiH	8-14	677	1.52	102	61
Be	201	1261	2.95	35.3	90
Al	210	660	4.36	8.9	243

For the rf windows we assume a fixed ratio of β_{\perp} with respect to that at the absorber. This ratio is given in the table of parameters.

For an extended channel with average momentum loss $\frac{dp}{d\ell}$

$$\epsilon_n = \epsilon_{\text{equilib}} + (\epsilon_{\text{initial}} - \epsilon_{\text{equilib}}) e^{-\frac{dp}{d\ell} \frac{\ell}{p}} \quad (5)$$

and the initial rate of emittance reduction is seen to be:

$$\left(\frac{1}{\epsilon_n} \frac{d\epsilon_n}{d\ell} \right)_{\text{initial}} = -\frac{1}{p} \frac{dp}{d\ell} \left(1 - \frac{\epsilon_{\text{equilib}}}{\epsilon_{\text{initial}}} \right) \quad (6)$$

3 Comparison with ICOOL

Figure 1 shows the cooling calculated from Eq. 5, and as simulated by ICOOL [5] for the SFOFO lattice being studied for the cooling experiment (MICE) [6]. One cell of the example uses 35 cm of liquid hydrogen, two 360 μm aluminum windows, and a total axial thickness of 2.5 mm (0.2 + 3 \times 0.7 + 0.2) of beryllium for the rf windows. The parameters used were as given in Tb. 2. For comparison, those for the final Study 2 cooling lattice are also given.

From Fig. 1, it is seen that the theoretical prediction of cooling is well reproduced by ICOOL.

4 Grids vs. Foils

At the start of the cooling channel there is a total of 2.5 mm of Be foils per cell. This is the thickness on axis. In Study 2 the foils are stepped, so that

Table 2: SFOFO lattice parameters used in the simulations of the MICE experiment.

lattice	(1,1)	(2,3)	
cell	2.75	1.65	m
F(E)	1.05	1.05	
p_{ave}	220	213	MeV/c
ϵ_o	8.9	2.2	π mm rad
Δp	13.14	7.9	MeV/c
β_{\perp}	40	18	cm
β_{rf}/β_{\perp}	2	3	

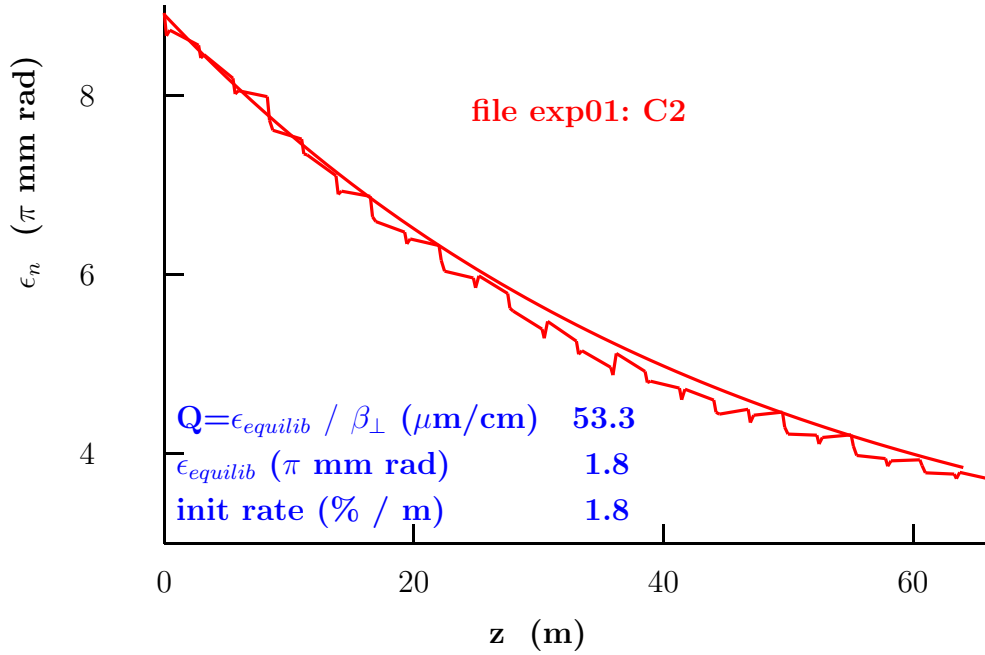


Figure 1: Cooling as a function of distance of the SFOFO lattice studied for the MICE experiment. We show the comparison of the analytical expression Eq. 5 and ICOOL simulation.

at the outer edges there is twice this thickness, but relatively few particles pass through this outer region, and its effect is not large.

If the center to center spacing of the tubes [7] in a grid is $f_{\text{spacing}} \times 2r$ then, on average, the wall thickness of aluminum tubes that would have the same scattering effect would be:

$$t_{\text{Al tube}} \approx \frac{L_{\text{Al}}}{L_{\text{Be}}} \frac{f_{\text{spacing}}}{\pi} \frac{\Sigma t_{\text{Be}}}{n_{\text{grids}}}, \quad (7)$$

for $\Sigma t_{\text{Be}} = 2.5$ mm, $f_{\text{spacing}} = 1.25$ (80% coverage), $n_{\text{grids}}=10$ (two planes for each boundary of 4 cavities, then the equivalent wall thickness is 24 μm .

This is a somewhat conservative estimate, since it ignores the effects of the greater Be thicknesses at the outer radii. It is also conservative in that grids might only be used between cavities, with Be foils used at the ends where the apertures are smaller, the heating down, and the required thickness less.

The average scattering from such tubes is less if their spacing is wider, but the surface fields will then be higher (approximately linear with the spacings divided by the diameter. Even with the tubes touching, there will be a significant field enhancement.

5 Calculations for Different Cases

Given this agreement, we can make calculation for other cases. Figure 2 shows values of calculated minimum emittance for $\beta_{\perp}=1$ cm, *i.e* Q' , as a function of the total thickness of aluminum windows, with LH, LHe and LiH. The continuous thin lines show results with Be rf windows. In the hydrogen case, the dashed lines show results without the rf windows, and the continuous thick line is for the case of 125 μm (5 mil) wall aluminum tubes, with 80% coverage, instead of the rf Be windows.

Particular values have been selected and marked on Fig. 2 and given in Tb. 3.

1. For hydrogen with no windows.
2. For hydrogen with aluminum absorber windows, but no Be rf windows.
3. For hydrogen with aluminum absorber windows, and Be rf windows, but no *safety* windows. This is the case in Study 2.

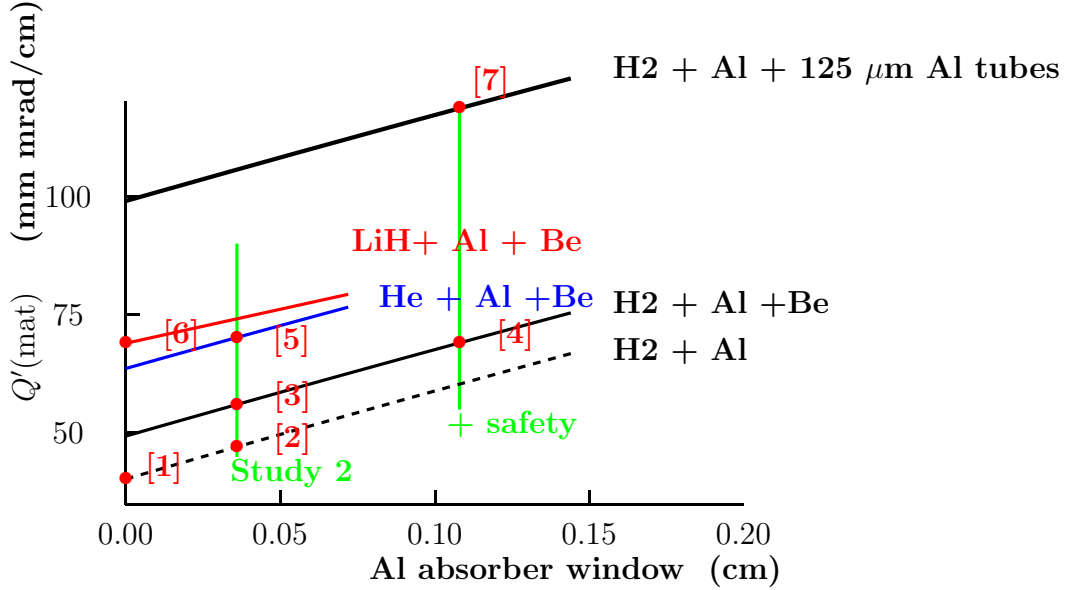


Figure 2: Calculated equilibrium emittance for $\beta_{\perp}=1$ cm, *i.e.* Q' , as a function of the total thickness of aluminum windows in cm. The lattice used correspond to the beginning of Study 2 cooling channel.

4. As in Study 2, but with aluminum safety windows twice the thickness of the primary windows, placed close to those primary windows. The doubling of the thickness corresponds to standard safety requirements, but their placement close to the primary windows does not. Larger, and thus thicker windows would be required if they were placed further from the hydrogen, and their effect would be greater because of rising β_{\perp} . On the other hand, it may be acceptable to make the safety windows of Be, which would reduce their effect.
5. For helium instead of hydrogen. The primary window is kept the same, but there is no safety window included.
6. For solid lithium hydride. No window is assumed. Some very thin window may be required to keep moisture out, but its effect is assumed to be insignificant.
7. For hydrogen with a safety window, but 125 μm (5 mil) aluminum tubes instead of the Be foils.

We note that in all cases, the changes in cooling rate are far less than

Table 3: Parameters of the different cases discussed in the text.

Material	L1 cm	L2 cm	L3 cm	Q'(mat) mm mrad/cm	$\epsilon_{\text{equilib}}$ mm	rate %/m
At Start	$\beta_{\perp}=0.35$ m			$\epsilon_{\text{initial}} = 8.9 \pi$ mm rad		
1) H2 only	19.3	0.000	0.000	40.3	1.73	1.79
2) H2 + Al	18.8	0.036	0.000	47.1	2.02	1.72
3) H2 + Al + Be rfw	17.5	0.036	0.125	56.1	2.40	1.62
4) H2 + Al+ Safety + Be rfw	16.4	0.108	0.125	69.1	2.96	1.48
5) He + Al + Be rfw	20.7	0.036	0.125	70.2	3.01	1.47
6) LiH + Be rfw	3.2	0.000	0.125	69.0	2.96	1.48
7) H2 + Al + Safety + 5 mil tubes	16.0	0.108	0.164	118.5	5.08	0.95

the changes in equilibrium emittance. This is because the emittance is much larger than this equilibrium emittance.

For the particular examples in Tb. 3, we note:

1. With only hydrogen and no windows, the equilibrium emittance is low (1.73 π mm rad), which is 1/5 of the assumed initial emittance. This leads to a cooling rate (1.79% /m) which is 4/5 of the ideal rate with no Coulomb scattering.
2. Adding the aluminum absorber windows raises the equilibrium emittance by 17%, and lowers the rate by 4%.
3. The use of Be rf windows raises the equilibrium emittance by another 20%, but lowers the initial cooling rate by only 6%.
4. The addition of safety hydrogen windows raise the equilibrium emittance by 23% compared with the Study 2 value, and lowers the cooling rate by 9%.
5. The equilibrium emittances and cooling rates for helium absorbers, assuming no need for safety windows, are essentially the same as those with solid LiH, and those with hydrogen with safety windows.

Table 4: Average $\frac{\mu}{p}$, errors and calculated cooling rate for the initial Study 2 cooling lattice. * Note that the second case is not the same as that discussed above. It is for LH and the Study 2 Al windows, but no rf windows.

Case	ave $\frac{\mu}{p}$	Initial Cooling Rate %/m
1) H2 only	0.157 ± 0.06	1.95
2* H2 + Al	0.148 ± 0.06	1.90
3) H2 + Al + rfw	0.139 ± 0.04	1.81
4) H2+Al+Safety+rf	0.127 ± 0.02	1.71
5) He + Al + rfw	0.121 ± 0.02	1.71
6) LiH + rfw	0.121 ± 0.02	1.61

- The use of 125 μm (5 mil) aluminum tubes and 80% coverage, instead of Be foils, raises the equilibrium emittance by a factor of 1.4 and lowers the cooling rate by 36%, which would presumably be unacceptable. Increasing the spacing by a factor of 5 would correct the problem, but increase the peak surface fields by the same factor.

6 ICOOL Simulations of Cases

To observe the effect of these cases on a Neutrino Factory, we made a number of simulations of the full Study 2 cooling channel. Each run used 5000 initial protons. Errors were estimated by observing the *rms* scatter of observed simulations using differing random starts. The resulting average $\frac{\mu}{p}$'s and their errors are given in Tb. 4, together with the calculated cooling rate for the first lattice. Note that the average $\frac{\mu}{p}$ is lower than the value published in Study 2. Part of this discrepancy is due to an error in the treatment of large angle scattering in ICOOL, which was discovered after the completion of Study 2 (we are using version 2.32 in the present simulations).

The results are shown in Fig. 3, and we see the same trend toward lower performance as the windows are introduced or increased in thickness.

It is interesting to compare these results with the calculated cooling rates for the first cooling lattice of Study 2. One observes an approximately linear relationship. Fig. 4 gives these $\frac{\mu}{p}$ results versus the calculated rates in the first cooling lattice. It is seen that there is indeed an approximately linear

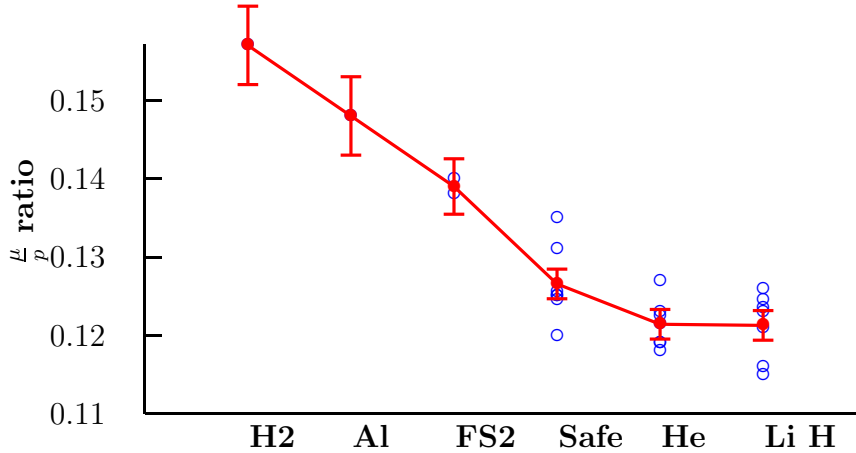


Figure 3: The average $\frac{\mu}{p}$ for the different cases considered in this paper.

relationship between them, but that the performance with LiH is a lot better than expected, and that with He a little worse. These results can be understood (as suggested by Kaplan [8]) by the distance dependence of the β_{\perp} from the center of the absorbers. This dependency $\beta_{\perp} = \beta_o + z^2/\beta_o$ is weak for the first lattice where $\beta_o = 0.4$ m, but stronger for later lattices where β_o is progressively less. As a result, the dependence of performance on the thickness of the absorbers is greater for the full channel than for the first lattice. This effect favors the thinner LiH and disfavors the somewhat thicker He.

7 Conclusion

We need to think carefully about the costs, safety and inconvenience versus the advantages of hydrogen absorbers in a Neutrino Factory, and consider helium or lithium hydride as alternatives.

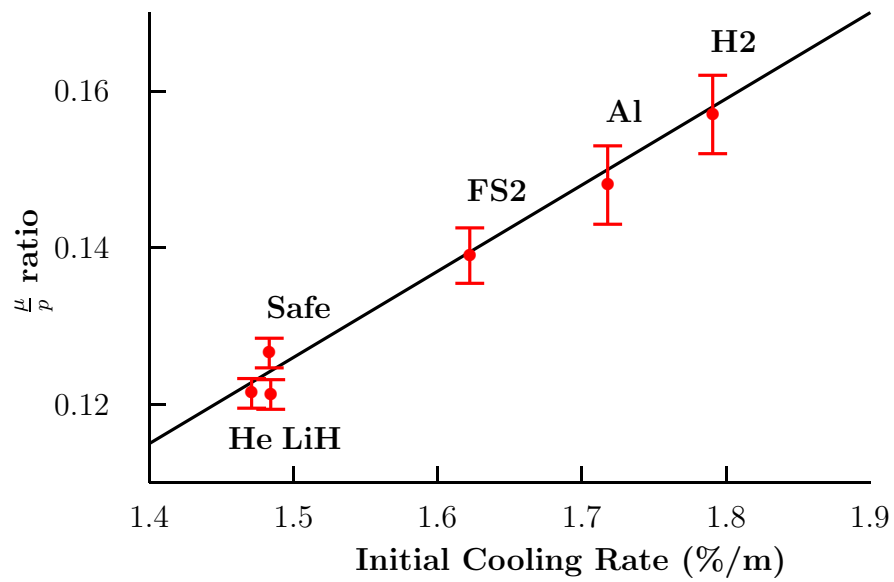


Figure 4: μ_p for the different cases considered in this paper vs. the calculated initial cooling rate.

References

- [1] *Feasability Study-II of a Muon-Based Neutrino Factory*, eds., S. Ozaki, R.B Palmer, M. Zisman and J.C. Gallardo, BNL-52623 (2001)
<http://www.cap.bnl.gov/mumu/studyii/FS2-report.html>
- [2] S. Pawel, private communication; R.E. Terry, *Lithium Hydride Debris Shields for Plasma Radiation Sources*, NRL/MR/6720-96-7868.
- [3] Cooling theory chapter of *Status of Muon Collider Research and Development and Future Plans*, Phys. Rev. ST Accel. Beams **2**, 081001.
http://www.cap.bnl.gov/mumu/pubs/status_report.html
- [4] *Review of Particle Physics*, Particle Data Group
<http://pdg.lbl.gov>
- [5] R. Fernow, *ICOOL: A simulation code for Ionization Cooling of Muon Beam*, Proc. Particle Accelerator Conference, 1999.
- [6] *MICE: International Muon Ionization Cooling Experiment*
<http://hep04.phys.iit.edu/cooldemo/>
- [7] Chapter 14 in reference [1]
- [8] D. Kaplan, Technical Board Meeting, IIT, Chicago , Feb. 2002.